

Articles

Homogeneous Nucleation of Water in Mesoporous Zeolite Cavities

A. H. Janssen,[†] H. Talsma,[‡] M. J. van Steenberg,[‡] and K. P. de Jong^{*,†}

Department of Inorganic Chemistry and Catalysis, Debye Institute, Utrecht University, P.O. Box 80083, 3508 TB Utrecht, The Netherlands, and Department of Biopharmacy and Pharmaceutical Technology, Utrecht University, Sorbonnelaan 16, 3584 CA Utrecht, The Netherlands

Received February 26, 2003. In Final Form: October 7, 2003

In this paper, we show that water inside mesoporous cavities in zeolites can be supercooled to ca. $-40\text{ }^{\circ}\text{C}$ at which point homogeneous nucleation of the water takes place. The fundamental phenomena observed here are similar to those reported earlier in for example emulsion droplets or droplets in the vapor phase. However, as these zeolite materials are widely available, they may provide an easily accessible source for studies of supercooled liquids in confinements. Next to this, it is now possible to discriminate with thermoporometry between mesoporous cavities inside the zeolite crystals, in which homogeneous nucleation takes place, and mesopores that are connected to the external surface in which heterogeneous nucleation takes place.

Introduction

With thermoporometry, mesoporosity can be assessed. It relies on the depression of the melting point of water (or another condensed adsorbate) due to the strong curvature of the solid–liquid interface present within small pores.¹ A full thermodynamic description of this phenomenon can be found in the literature.^{2,3} In a differential scanning calorimeter (DSC), the sample is first strongly cooled, after which the heat flux upon heating is studied as a function of temperature. The depression of the melting point of water, $\Delta T\text{ (}^{\circ}\text{C)} < 0$, is related to the pore radius, r (nm), by a modified Gibbs–Thomson relation:^{4,5}

$$r = A - B/\Delta T \quad (1)$$

For heating scans, $A = 0.68\text{ nm}$ and $B = 32.33\text{ nm K}$ are used, while for cooling scans $A = 0.57\text{ nm}$ and $B = 64.67\text{ nm K}$ are used.⁴ The above-mentioned values for A consist of a.o. a correction for a nonfreezing layer of 0.8 nm adsorbed on the walls of the pores. Different values for the thickness of the nonfreezing layer and for A and B are sometimes used in the literature,^{6–9} but the above-mentioned values are most commonly used. In principle,

both the freezing point depression and the melting point depression can be used to determine the pore radius; however, delayed nucleation can have a large influence on the calculated pore radii calculated from the freezing-point depression. Therefore, the melting point depression is more reproducible and most often used.¹

The above holds for heterogeneously nucleated ice. Upon cooling of a porous network, ice present at the pore ends offers nucleation sites for the water in the mesopores to freeze. However, water can also freeze via homogeneous nucleation. If pure water is supercooled to ca. $-38\text{ }^{\circ}\text{C}$, the thermodynamic properties of this supercooled water change rapidly, forcing the system to nucleate.^{10–15,23} Such high degrees of supercooling require small isolated water droplets that have been obtained in atmospheric studies,¹³ cloud chamber experiments,¹⁴ or emulsions.²³

Zeolites are microporous crystalline aluminosilicates, which makes them very suitable for separation processes or shape selective catalysis.¹⁶ In catalysis, the micropores, with diameters between 0.3 and 1.2 nm , can induce shape selectivity. However, diffusion of products and reactants in the micropores is slow. To increase the transport of molecules through the zeolite crystals, mesopores are

* To whom correspondence should be addressed. E-mail: k.p.dejong@chem.uu.nl.

[†] Department of Inorganic Chemistry and Catalysis, Debye Institute.

[‡] Department of Biopharmacy and Pharmaceutical Technology.

(1) Cuperus, F. P.; Bargeman, D.; Smolders, C. A. *J. Membr. Sci.* **1992**, *66*, 45.

(2) Iza, M.; Woerly, S.; Danumah, C.; Kaliaguine, S.; Bousmina, M. *Polymer* **2000**, *41*, 5885 and references therein.

(3) Jallut, C.; Lenoir, J.; Bardot, C.; Eyraud, C. *J. Membr. Sci.* **1992**, *68*, 271.

(4) Brun, M.; Lallemand, A.; Quinson, J. F.; Eyraud, C. *Thermochim. Acta* **1977**, *21*, 59.

(5) Hay, J. N.; Laity, P. R. *Polymer* **2000**, *41*, 6171.

(6) van Bommel, M. J.; den Engelsens, C. W.; van Miltenburg, J. C. *J. Porous Mater.* **1997**, *4*, 143.

(7) Schreiber, A.; Ketelsen, I.; Findenegg, G. H. *Phys. Chem. Chem. Phys.* **2001**, *3*, 1185.

(8) Schmidt, R.; Hansen, E. W.; Stoecker, M.; Akporiaye, D.; Ellestad, O. H. *J. Am. Chem. Soc.* **1995**, *117*, 4049.

(9) Ishikiriyama, K.; Todoki, M.; Motomura, K. *J. Colloid Interface Sci.* **1995**, *171*, 92.

(10) Franks, F. *Water, a Comprehensive Treatise. Volume 7: Water and Aqueous Solutions at Subzero Temperatures*; Plenum Press: New York, 1982.

(11) Angell, C. A.; Oguni, M.; Sichina, W. J. *J. Phys. Chem.* **1982**, *86*, 998.

(12) Bergman, R.; Swenson, J. *Nature* **2000**, *403*, 283.

(13) Rosenfeld, D.; Woodley, W. L. *Nature* **2000**, *405*, 440.

(14) Kraemer, B.; Huebner, O.; Vortisch, H.; Woeste, L.; Leisner, T.; Schwell, M.; Ruehl, E.; Baumgaertel, H. *J. Chem. Phys.* **1999**, *111*, 6521.

(15) Pruppacher, H. R. *J. Atmos. Sci.* **1995**, *52*, 1924.

(16) Marcilly, C. R. *Top. Catal.* **2000**, *13*, 357.

Table 1. Nitrogen Physisorption Results

sample	V_{micro} (mL/g) ^a	V_{meso} (mL/g) ^b	V_{cavities} (mL/g) ^c	S_{ext} (m ² /g) ^d	mesopore	
					diam (nm) ^e	% cavities
NaY	0.34	0	0	8		
USY	0.26	0.04	0.01	63	4–20	20
XVUSY	0.28	0.12	0.05	120	4–40	29
HMVUSY	0.15	0.26	0.02	146	4–25	7
MCM41	0	0.97	0	996	2.8	

^a From *t*-plot. ^b Mesopore volume of cylindrical mesopores with diameters specified in the sixth column. ^c Volume of the mesoporous cavities. ^d Sum of external and mesopore surface area from *t*-plot. ^e Calculated from the desorption isotherm using the BJH method [ref 22].

created in the crystals by steam and/or acid treatments. These mesopores, with diameters between 2 and 50 nm, can act as highways for diffusion to the interior of the zeolite crystal, thereby decreasing the path length for diffusion in the micropores. Recently, we found that for steamed Y zeolite up to 30 vol % of the mesopores were cavities inside the crystals that are connected to the external surface via the micropore system only.^{17,18} These cavities are most likely less effective in enhancing molecular transport in the zeolite crystals.

In this paper, we show that water inside mesoporous cavities in zeolites can be supercooled to ca. $-40\text{ }^{\circ}\text{C}$ at which point homogeneous nucleation of the water takes place. As these materials are widely available, they may provide an easily accessible source for the study of supercooled liquids in confinements. Next to this, it is now possible to discriminate with thermoporometry between mesoporous cavities inside the zeolite crystals, in which homogeneous nucleation takes place, and mesopores that are connected to the external surface in which heterogeneous nucleation takes place.

Experimental Section

Materials. For this study, a series of Y zeolites with increasing mesopore volumes were used. Samples of NaY (CBV100), Ultra Stable Y (USY, CBV400), eXtra Very Ultra Stable Y (XVUSY, CBV780) and High-Meso Very Ultra Stable Y (HMVUSY) were obtained from Shell International Chemicals. NaY was used as a reference material, while USY, an NH_4Y steamed at typically $550\text{ }^{\circ}\text{C}$, was chosen for its well-confirmed presence of mesopores. XVUSY is typically prepared by steaming of NH_4Y at $550\text{ }^{\circ}\text{C}$, followed by a second steaming step at higher temperatures, for example, $750\text{ }^{\circ}\text{C}$, and finally acid leaching to obtain the desired Si/Al ratio. The hydrothermal treatment for the synthesis of HMVUSY consists typically of contacting a dealuminated zeolite Y with a unit cell size of 2.437 nm with an aqueous solution of 6 N NH_4NO_3 at a pH between 3 and 7 at $150\text{ }^{\circ}\text{C}$ for 6 h in a pressure equipment. During the hydrothermal treatment, the aqueous solution stays partially in the liquid state.¹⁹ Since the reference material NaY does not contain any mesopores, a sample of MCM-41 was used as a second reference material. The synthesis of the MCM-41 sample with CTABr as a template has been described in the literature.²⁰ In Table 1, the results of a previous characterization study of the zeolite samples with nitrogen physisorption are given.¹⁷

Thermoporometry. Samples were prepared by adding water to the dry materials until a thick suspension had been obtained, which was left in a closed cup for at least 24 h to allow the water

Table 2. Bulk Water Freezing Temperatures

$T\text{ (}^{\circ}\text{C)}$	sample					
	water	NaY	USY	XVUSY	HMVUSY	MCM-41
	-21.2	-17.5	-15.2	-8.5	-15.4	-17.7

to penetrate in the pores. The amount of water was ca. 3 times the total pore volume determined with nitrogen physisorption. For the DSC cooling and heating scans, samples of 10–40 mg of the suspensions were measured on a TA Instruments DSC Q1000 using a rate of $0.5\text{ }^{\circ}\text{C}/\text{min}$. With heating and cooling rates up to $0.5\text{ }^{\circ}\text{C}/\text{min}$, the position and shape of the DSC peaks appeared independent of the scanning rate, while scanning rates above $0.5\text{ }^{\circ}\text{C}/\text{min}$ resulted in a shift of the peak positions. After cooling the sample at $0.5\text{ }^{\circ}\text{C}/\text{min}$ to $-60\text{ }^{\circ}\text{C}$, several subsequent heating and cooling scans were recorded from -60 to $-2\text{ }^{\circ}\text{C}$ and vice versa. The lower temperature limit of $-2\text{ }^{\circ}\text{C}$ was chosen to keep the bulk water frozen while the ice in the mesopores was molten.

The peak onset was defined as the point where the measured curve, after subtraction of the curve of NaY, started to deviate from a linear background. After subtraction of the background, pore volumes were calculated by integrating the peaks while using the heating rate and the temperature dependence of both the density of ice⁹ and the enthalpy of fusion.⁴

Results

Before the heat flows were measured during heating and cooling, the sample was first cooled to $-60\text{ }^{\circ}\text{C}$ in order to freeze all the water in the system. The temperatures at which the bulk water froze in this first cooling step are given in Table 2. From this table, it is clear that despite a cooling rate of $0.5\text{ }^{\circ}\text{C}/\text{min}$ the bulk water froze with a substantial supercooling indicating that the water was very pure. The bulk water freezing temperature was several degrees higher when material was present compared to only water which might indicate that the zeolite particles provide nucleation sites for the ice crystals. Still, there was a substantial supercooling even in the presence of zeolite particles.

In Figure 1, the DSC curves of the four zeolite samples are given together with the DSC curves of water and MCM-41 which were used as reference materials. All curves show a slope due to the heat capacity of the zeolite–water/ice system. As can be concluded from Figure 1A, no peaks are present for pure water upon warming of the completely frozen sample (from -60 to $-2\text{ }^{\circ}\text{C}$). With the other five samples, a peak is coming up at ca. $-2\text{ }^{\circ}\text{C}$ which is due to the melting of the water in the intercrystalline spaces. For NaY, no additional peaks are present as there are no mesopores in this material. For USY, XVUSY, HMVUSY, and MCM-41, additional peaks at ca. $-10\text{ }^{\circ}\text{C}$ (zeolite samples) and $-40\text{ }^{\circ}\text{C}$ (MCM-41) are obtained, which are due to the melting of the water in the mesopores of the materials. After cooling of the samples with the bulk water still frozen (from -2 to $-60\text{ }^{\circ}\text{C}$, see Figure 1B), there are no peaks for pure water. The other five samples show a peak around $-2\text{ }^{\circ}\text{C}$, which is due to the freezing of the water in the intercrystalline spaces. For NaY, no other peaks are present, but additional peaks are present for both MCM-41 and the three mesoporous zeolite samples due to the freezing of water in the mesopores. In Table 3, the onset temperatures and relative areas of the peaks are given. The onsets of the peaks in the exotherm at $-16.5\text{ }^{\circ}\text{C}$ for USY, $-5.9\text{ }^{\circ}\text{C}$ for XVUSY, and $-11.8\text{ }^{\circ}\text{C}$ for HMVUSY could not be determined exactly due to the overlap with the peak at $-2\text{ }^{\circ}\text{C}$. Instead, the temperature at the minimum between the peak at $-2\text{ }^{\circ}\text{C}$ and the peak at $-16.5\text{ }^{\circ}\text{C}$ was taken for USY ($-9.0\text{ }^{\circ}\text{C}$). Analogously, the onsets of the peaks in the exotherm of XVUSY and HMVUSY were determined to be -3.9 and $-7.0\text{ }^{\circ}\text{C}$, respectively.

(17) Janssen, A. H.; Koster, A. J.; de Jong, K. P. *J. Phys. Chem. B* **2002**, *106*, 11905.

(18) Janssen, A. H.; Koster, A. J.; de Jong, K. P. *Angew. Chem., Int. Ed.* **2001**, *40*, 1102.

(19) Cooper, D. A.; Hastings, T. W.; Hertzberg, E. P. U.S. Patent 5,601,798, 1997.

(20) Lensveld, D. J.; Mesu, J. G.; van Dillen, A. J.; de Jong, K. P. *Microporous Mesoporous Mater.* **2001**, *44–45*, 401.

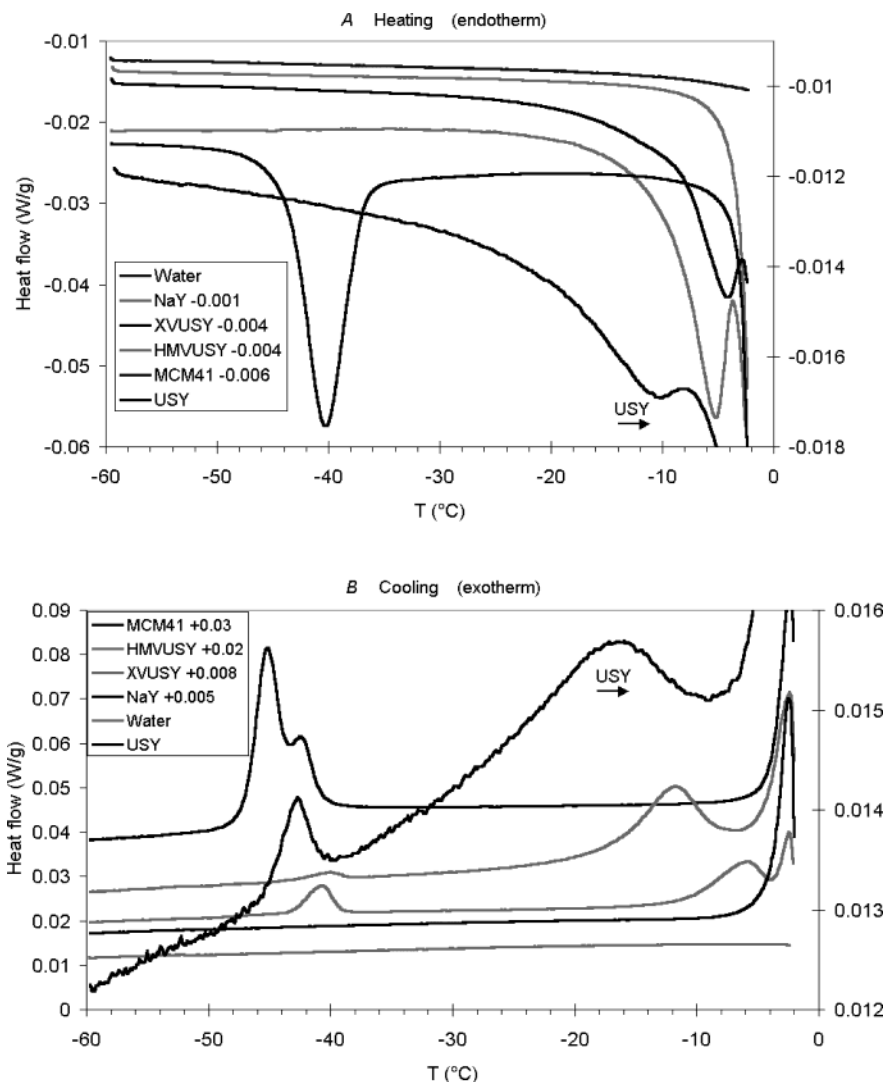


Figure 1. DSC curves (heat flow vs temperature) during warming (A) and cooling (B) of water, NaY, XVUSY, HMVUSY, and MCM-41 (left axis) and USY (right axis). For clarity, some of the curves have been shifted upward or downward. The order of the samples in the legend (from top to bottom) is the order of the curves at the left side of the graphs.

Discussion

With thermoporometry, usually the endotherm (heating scan) is used to determine pore diameters. Since NaY has no mesopores, MCM-41 with its well-defined cylindrical pore system with a sharp pore size distribution was used as a reference to test the peak positions. The MCM-41 sample had uniform pore diameters of 2.8 nm (as determined with the Barrett–Joyner–Halenda (BJH) method from nitrogen desorption data) which is very close to the 2.7 nm found from the analysis of the peak onset in the endotherm ($-50\text{ }^{\circ}\text{C}$) using the Gibbs–Thomson relation of eq 1 (see Figure 1A and Table 2). The peak in the endotherm has a maximum at $-40.3\text{ }^{\circ}\text{C}$, which corresponds to a pore diameter of 3.0 nm. This indicates that the pore size distribution as derived from the thermoporometry data is broader than that calculated from the nitrogen desorption isotherm. Therefore, it is not surprising that the mesoporous zeolites, which have a broad pore size distribution according to the BJH method of the nitrogen desorption data, give a very broad peak in the endotherm and exotherm. At the high-temperature end, the peak overlaps with the peak of water in the intercrystalline spaces. This makes it difficult to draw any conclusion from these thermoporometry data about the upper limit of the mesopore diameters. Nonetheless, the diameter calculated from the onsets of the peaks in

the endotherm, the diameters calculated from the peak maxima in the endotherm, and the large peak widths, which suggest broad pore size distributions, are in good agreement with the nitrogen physisorption data.

The exotherm of MCM-41 shows two overlapping peaks, whereas the endotherm shows only one peak. This phenomenon has been observed before, although no explanation was found.⁷ One possible explanation could lie in a combined heterogeneous and homogeneous nucleation. Due to the very small pore diameter, the heterogeneous nucleation of the water in the mesopores occurs at temperatures at which homogeneous nucleation comes into play. Heterogeneous nucleation, however, dominates with MCM-41, since the peaks in the exotherm and the endotherm largely overlap. For the mesoporous zeolites, strong evidence for homogeneous nucleation is discussed hereafter.

In the exotherm of USY, two peaks are visible (at ca. -17 and $-43\text{ }^{\circ}\text{C}$), whereas the endotherm shows only one peak (at ca. $-10\text{ }^{\circ}\text{C}$). The two peaks in the exotherm can be explained with two theories. The first one is based on a bimodal pore size distribution with mesopores of the dimensions of the pores in MCM-41 (peak at $-43\text{ }^{\circ}\text{C}$) and larger mesopores (peak at $-17\text{ }^{\circ}\text{C}$). In that case, however, one would expect also two peaks in the endotherm: one around $-40\text{ }^{\circ}\text{C}$ (just like MCM-41) and one at much higher

Table 3. Peak Onsets, Peak Maximums, and Peak Areas of the Heating and Cooling DSC Curves of USY, XVUSY, HMVUSY, and MCM-41

sample	T_{onset} (°C) ± 2 °C	pore D (nm) ^a	T_{max} (°C)	pore D (nm) ^a	peak area (J/g)	pore volume (mL/g) ^b
Heating (Endotherm)						
USY ^c	-34	3	-10.5	7.5	2.3	0.033
USY ^d	-28	4	-10.4	7.6	2.0	0.028
XVUSY ^c	-32	3	-4.1	17.1	14.7	0.18
XVUSY ^d	-30	4	-4.1	17.1	12.0	0.14
HMVUSY ^c	-25	4	-5.3	13.6	18.5	0.24
HMVUSY ^d	-25	4	-5.3	13.6	18.0	0.23
MCM-41	-50	2.7	-40.3	3.0	16.3	0.62
Cooling (Exotherm)						
USY	-9.0 ^e	>15.5	-16.5	9.0	n.d. ^g	
	-40.1	n.p. ^f	-42.7	n.p. ^f	0.3	
XVUSY	>-3.9 ^e	>34.3	-5.9	23.1	n.d. ^g	
	-38.2	n.p. ^f	-40.7	n.p. ^f	2.1	
HMVUSY	>-7.0 ^e	>19.6	-11.8	12.1	n.d. ^g	
	-38.2	n.p. ^f	-40.2	n.p. ^f	0.6	
MCM-41	-38.5	4.5	-42.5	4.2	15.9	

^a Calculated with eq 1. ^b Calculated by correcting the peak area for the density of ice and the enthalpy of fusion. ^c Heating from -60 to -2 °C. ^d Heating from -35 to -2 °C after cooling from -2 to -35 °C. ^e Not exactly determined due to overlap with the peak at -2 °C. ^f n.p. = not possible to determine with eq 1 due to homogeneous nucleation; see the text. ^g n.d. = not determined due to overlap with the peak at -2 °C.

temperatures (like the one that is observed in the endotherm of USY). In the second approach, it is assumed that the peak at -17 °C is caused by heterogeneous nucleation in the mesopores and that the peak at -43 °C is caused by homogeneous nucleation. The heterogeneous nucleation can be explained as follows. At -2 °C, the system consists of zeolite particles with liquid water in the pores, while the bulk water is still frozen. Upon cooling, first the water in the large mesopores between the zeolite crystals freezes, leading to a system of zeolite particles completely surrounded by ice. This ice offers nucleation sites for water in the cylindrical mesopores that extend to the external surface of the zeolite crystals. As soon as the temperature is low enough for ice to be stable in the confined space of these mesopores, the water in these mesopores starts to freeze from these nucleation sites. However, for water in mesoporous cavities that are connected to the external surface by the very small micropores only the situation is different. This water is not in contact with any ice crystals that could serve as nucleation sites. Upon cooling, the statistical chance of forming stable ice nuclei (homogeneous nucleation) is very low due to the small volume of the individual cavities.¹⁵ Due to this, the water in the cavities is supercooled. Around -38 °C, the properties of supercooled water change very fast, forcing the system to nucleate.^{10-15,23} The onset of the homogeneous nucleation peak is also a function of the size of the pores.²¹ However, the temperature regime is only a few degrees Celsius and no reference data for pores below 150 nm were found. Therefore, it was not possible to derive pore size information from this peak position. Upon heating, the modified Gibbs-Thomson relation of eq 1 holds. Since both the cavities and the cylindrical mesopores are of about the same pore sizes, only a single peak is found in the endotherm.

In an additional experiment, first the system was cooled at 0.5 °C/min from -2 to -35 °C and subsequently heated at 0.5 °C/min to -2 °C. The pore volume calculated from the peak area in the endotherm was lower than when the system was heated from -60 to -2 °C (see Table 3). According to the proposed theory, only heterogeneously nucleated ice is present at -35 °C. Because the water in the cavities is still in the liquid state, it does not have to melt upon heating, which leads to a lower heat flow detected than when the system is heated from -60 °C and also the ice in the cavities melts. Analogously, the system was cooled to -60 °C (the peak at -43 °C was present in the exotherm) after which a cycle of heating (to -35 °C) and cooling (to -60 °C) was performed. In neither the heating (-60 to -35 °C) nor in the second cooling step (-35 to -60 °C) was any heat flow detected. This further supports the theory that the heat released in the first cooling step (the peak at -43 °C) corresponds to part of the heat input that is measured in the single peak in the endotherm (at ca. -10 °C).

Since the peak at -43 °C is due to homogeneous nucleation in the cavities and not in the cylindrical mesopores, the relative volume fraction of cavities can be calculated from the pore volumes calculated from the two peaks in the exotherm. However, as the peak due to the homogeneous nucleation lies around -40 °C there is a very large uncertainty in the calculated pore volume as the enthalpy of fusion changes rapidly at these temperatures and its exact value around -40 °C is not well-known. The difference in the pore volumes calculated from the endotherm when heating from -35 to -2 °C and from -60 to -2 °C also corresponds to the pore volume of the cavities. Therefore, the relative volume fraction of cavities can also be calculated from the peaks in the endotherm. The relative volume fraction of cavities thus calculated for the USY material is 15% (1 - 0.028/0.033). This value is in good agreement with the fraction determined with nitrogen physisorption (20%, Table 1). Qualitatively, the homogeneous nucleation induced peak in the thermoporometry measurements strongly supports the presence of cavities in steamed zeolite Y crystals.

Analogously, the relative volume fractions of cavities can be calculated for XVUSY and HMVUSY and amount to 22% and 4%, respectively. Also, these two values are in good agreement with the 29% and 7% determined with nitrogen physisorption.

For USY, XVUSY, and HMVUSY, the volumes of the cylindrical mesopores calculated from the thermoporometry data (0.028, 0.14, and 0.23 mL/g, see Table 3) are in good agreement with the volumes calculated with nitrogen physisorption (0.04, 0.12, and 0.26 mL/g, see Table 1). For MCM-41, however, the pore volume calculated with thermoporometry (0.62 mL/g) is much lower than the mesopore volume determined with nitrogen physisorption (0.97 mL/g). This difference is most likely due to uncertainties in the value of the enthalpy of fusion at -40 °C.

The value of the enthalpy of fusion (ΔH_f^{-40}) around -40 °C can be estimated with the formula

$$\Delta H_f^{-40} = 18Q/(V\rho_{\text{ice}}) \quad (2)$$

where the value 18 is the atomic mass of water, ρ_{ice} is the density of ice (a value of 0.92 g/mL is taken), Q is the area of the peak around -40 °C in the exotherm in J/g (see Table 3), and V is the volume of the mesoporous cavities in mL/g (see Table 1). Thus calculated values of 587, 822, and 587 J/mol for the data of USY, XVUSY, and HMVUSY, respectively, are obtained. The error margin in the values of Q is estimated at 20% (based on the difference in peak

(21) Talsma, H.; van Steenberg, M. J.; Crommelin, D. J. A. *Cryobiology* **1992**, *29*, 80.

(22) Barret, P.; Joyner, L. G.; Halenda, P. P. *J. Am. Chem. Soc.* **1951**, *73*, 373.

(23) Bartell, L. S. *Annu. Rev. Phys. Chem.* **1998**, *49*, 43.

area for the cavities between the exotherm and the endotherm), while a 10% error margin in the nitrogen volumes is assumed. Therefore, the actual value of the enthalpy of fusion around $-40\text{ }^{\circ}\text{C}$ is estimated to be around 680 J/mol .

Conclusions

Water inside mesoporous cavities in zeolites can be supercooled to ca. $-40\text{ }^{\circ}\text{C}$ at which point homogeneous

nucleation of the water takes place. Using thermoporometry, it is possible to discriminate between mesoporous cavities inside the zeolite crystals, in which homogeneous nucleation takes place, and mesopores that are connected to the external surface in which heterogeneous nucleation takes place. The results are in good agreement with results from nitrogen physisorption experiments.

LA034340K